Published in "Nature doi: 10.1038/nature10873, 2012"
which should be cited to refer to this work.

A petunia ABC protein controls strigolactone-dependent symbiotic signalling and branching

Tobias Kretzschmar[1], Wouter Kohlen[2]*, Joelle Sasse[1]*, Lorenzo Borghi[1], Markus Schlegel[1], Julien B. Bachelier[1], Didier Reinhardt[3], Ralph Bours[2], Harro J. Bouwmeester[2,4] & Enrico Martinoia[1]

Strigolactones were originally identified as stimulators of the germination of root-parasitic weeds[1] that pose a serious threat to resource-limited agriculture[2]. They are mostly exuded from roots and function as signalling compounds in the initiation of arbuscular mycorrhizae[3], which are plant–fungus symbionts with a global effect on carbon and phosphate cycling[4]. Recently, strigolactones were established to be phytohormones that regulate plant shoot architecture by inhibiting the outgrowth of axillary buds[5,6]. Despite their importance, it is not known how strigolactones are transported. ATP-binding cassette (ABC) transporters, however, are known to have functions in phytohormone translocation[7–9]. Here we show that the *Petunia hybrida* ABC transporter PDR1 has a key role in regulating the development of arbuscular mycorrhizae and axillary branches, by functioning as a cellular strigolactone exporter. *P. hybrida pdr1* mutants are defective in strigolactone exudation from their roots, resulting in reduced symbiotic interactions. Above ground, *pdr1* mutants have an enhanced branching phenotype, which is indicative of impaired strigolactone allocation. Overexpression of *Petunia axillaris PDR1* in *Arabidopsis thaliana* results in increased tolerance to high concentrations of a synthetic strigolactone, consistent with increased export of strigolactones from the roots. PDR1 is the first known component in strigolactone transport, providing new opportunities for investigating and manipulating strigolactone-dependent processes.

Strigolactones are a new class of carotenoid-derived[10] phytohormone in land plants. In addition to their role in shoot branching, strigolactones are exuded into the rhizosphere under phosphorus-limiting conditions[5] and act as growth stimulants of arbuscular mycorrhizal fungi[3]. To identify efflux carriers of arbuscular-mycorrhiza-promoting factors such as strigolactones, we used a degenerate primer approach (Supplementary Fig. 2a) to isolate full-size PDR-type transporters (also known as ABC subtype G (ABCG) transporters) of *P. hybrida* that are abundant in phosphate-starved or mycorrhizal roots. The rationale behind the focus on these transporters, of which there are 15 in *Arabidopsis*[11], 23 in *Oryza sativa* (rice)[11] and 23 putative factors in *Solanum lycopersicum* (tomato) (Supplementary Fig. 3a), was that they are plasma membrane proteins often found in roots[12], they are implicated in below-ground plant–microbe interactions[13,14], and they have affinities for compounds that are structurally related to strigolactones[8,9,15]. Of six primary candidates, only *P. hybrida PDR1* had increased expression in roots that were subjected to either phosphate starvation (Fig. 1a) or colonization by the arbuscular mycorrhizal fungus *Glomus intraradices* (Fig. 1b). Furthermore, *PDR1* transcript levels increased in response to treatment with the synthetic strigolactone analogue GR24 or the auxin analogue 1-naphthaleneacetic acid (NAA) (Fig. 1c). Auxin has been shown to upregulate strigolactone-biosynthesis genes[16] and to be involved in pre-symbiotic and early mycorrhizal events[17].

P. hybrida PDR1 is predicted to encode a full-size PDR cluster I protein (GenBank accession number JQ292813; Supplementary Figs 2b–c and 3b). The closest *Arabidopsis* homologue, ABCG40 (also known as PDR12), transports abscisic acid (ABA)[9]. However, in contrast to *Arabidopsis ABCG40*, *P. hybrida PDR1* is not regulated by ABA (Fig. 1c). A 1.8-kilobase (kb) element upstream of *PDR1* (GenBank

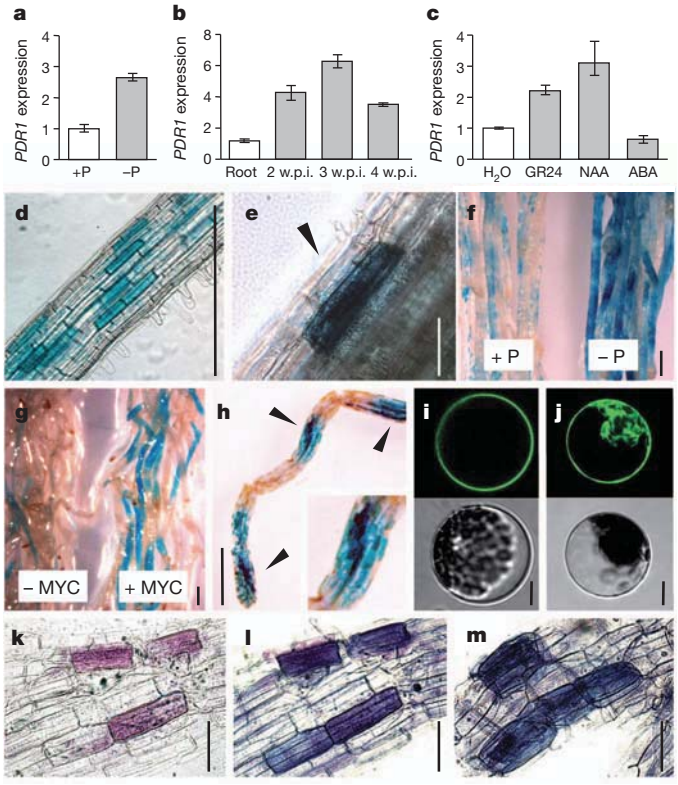

Figure 1 | Below-ground *PDR1* expression and PDR1 localization. **a–c**, Quantitative PCR for *PDR1* in W115 roots: in the presence or absence of phosphate (P) (**a**); at 2–4 weeks post inoculation (w.p.i.) with *G. intraradices* (**b**); and in response to water (H_2O), GR24, NAA or ABA (**c**). Data are presented as mean ± s.e.m. ($n = 3$, where n denotes the number of samples). **d–h**, The *pPhPDR1*::*GUS* signal in W115 roots without treatment (**d**, **e**) (black arrowheads indicate epidermal cells); under phosphate-sufficient and phosphate-deficient conditions (**f**); in response to mycorrhization (+MYC, 8 w.p.i.) (**g**); and in mycorrhized roots (8 w.p.i.) costained with black ink (**h**). Scale bars, 1 mm (**d**, **f–h**) and 0.1 mm (**e**). **i**, **j**, Transient CaMV *35S*::*GFP*::*gPaPDR1* expression in *Arabidopsis* mesophyll protoplasts. The *GFP*::*gPaPDR1* signal (**i**, top) and the corresponding transmission electron micrograph (**i**, bottom) and the free GFP signal (**j**, top) and transmission image (**j**, bottom) are shown. Scale bars, 10 μm. **k–m**, *pPhPDR1*::*GUS* signal co-localization with trypan-blue-stained root HPCs. Shown are a magenta GUS-stained root section (**k**), an additional trypan blue stain of the same sample (**l**) and stained wild-type root HPCs (**m**). Scale bars, 0.1 mm.

[1]Institute of Plant Biology, University of Zurich, 8008 Zurich, Switzerland. [2]Laboratory of Plant Physiology, Wageningen University, 6700 AR Wageningen, The Netherlands. [3]Department of Biology, University of Fribourg, 1700 Fribourg, Switzerland. [4]Centre for Biosystems Genomics, PO Box 98, 6700 AB Wageningen, The Netherlands.
*These authors contributed equally to this work.

accession number JQ292814) was fused to the GUS reporter and stably transformed into the *P. hybrida* cultivar W115. Below ground, *pPhPDR1*::*GUS* (promoter *P. hybrida PDR1–GUS* construct) expression was substantial in individual subepidermal cells of the lateral roots (Fig. 1d, e). These cells were largely identical to hypodermal passage cells (HPCs) (Fig. 1k–m), which are devoid of suberin and serve as cortical entry points for arbuscular mycorrhizal hyphae[18]. GUS staining was more prominent in roots grown under phosphate-deficient conditions (Fig. 1f) and in mycorrhizal roots, particularly in regions containing or flanking fully developed arbuscular mycorrhizal structures (Fig. 1g, h). These results suggested a role for PDR1 in arbuscular mycorrhiza during pre-symbiotic development and during intraradical colonization. To assess the localization of the PDR1 protein, the genomic *PDR1* orthologue from the *P. hybrida* progenitor *P. axillaris* (which has 99.7% amino acid identity to *P. hybrida* PDR1; GenBank accession number JQ292812; Supplementary Fig. 2b) was fused to the carboxy-terminus-encoding region of the green fluorescent protein (*GFP*) gene (*GFP*::*gPaPDR1*). Transient expression of *GFP*::*gPaPDR1* in *Arabidopsis* showed that PDR1 localizes to the plasma membrane (Fig. 1i, j), consistent with a role in secretion.

For functional analysis, we screened the dTph*1* transposon-containing *P. hybrida* line W138 for insertional *pdr1* mutants. A PCR-based DNA library screen of 1,000 individuals led to the identification of a dTph*1* insertion in exon 4 of *P. hybrida PDR1* (Supplementary Fig. 4a–d), together with a footprint allele causing a frame shift (Supplementary Fig. 4e). Insertion of dTph*1* in the coding region of a gene frequently results in a complete loss of function[19].

The W138 line with the mutant *pdr1* gene (W138-*pdr1*) was compared directly with W138 and was crossed with *P. hybrida* W115 for further segregation analysis. Five homozygous *pdr1* mutant lines (W115 × W138-*pdr1*) and wild-type lines (W115 × W138) were derived from the F_2 generation (Supplementary Fig. 4d). Phenotypes cosegregated with the mutation in *PDR1*, and transposon display analysis did not uncover other cosegregating dTph*1* insertions in the W115 × W138 lines (Supplementary Fig. 4f), suggesting that dTph*1* insertion in *PDR1* is responsible for the observed phenotypes. In addition, *P. hybrida PDR1* knockdown lines (*pdr1*-RNAi), which were created in W115 by using two independent RNA interference (RNAi) constructs (Supplementary Fig. 5a, b), showed similar phenotypes.

W138-*pdr1* had a significantly reduced ability to accommodate *Gigaspora margarita* and *G. intraradices* (Fig. 2a), two distantly related arbuscular mycorrhizal fungi with different growth strategies[4]. This finding indicated that PDR1 functions as a transporter of a stimulatory molecule involved in symbiosis with diverse arbuscular mycorrhizal fungal species. Indeed, root exudates from W138-*pdr1* showed reduced activity for stimulating the hyphal branching of *G. margarita* in an *in vitro* bioassay (Fig. 2b). Because these results suggested an involvement of strigolactones, W115 × W138-*pdr1* root exudates were assessed for their ability to stimulate the germination of the root-parasitic weed *Phelipanche ramosa* (Orobanchaceae). As a control, root exudates of *dad1* mutants from the *P. hybrida* cultivar V26 were used. *DAD1* encodes carotenoid cleavage dioxygenase 8 (CCD8)[20] and is an orthologue of the established strigolactone-biosynthesis genes *RMS1*, *MAX4* and *D10* in *Pisum sativum* (pea), *Arabidopsis* and rice, respectively[5,6]. The germination rate of *P. ramosa* was significantly lower in the presence of root exudates from W115 × W138-*pdr1* or *dad1* mutants than root exudates from the corresponding wild-type plants, which induced germination to a similar extent to GR24 (Fig. 2d). Comparable results were obtained with *pdr1*-RNAi lines (Supplementary Fig. 5c). When inoculated with *G. intraradices*, W115 × W138-*pdr1* lines had similarly retarded colonization rates to W138-*pdr1* and *dad1* mutants (Fig. 2c).

Despite the delay in arbuscular mycorrhizal development, neither W115 × W138-*pdr1* nor *dad1* mutants had any morphological aberrations in intracellular mycorrhizal structures (Fig. 2e–h). Intraradical hyphae and arbuscules appeared normal, suggesting that the quantitative

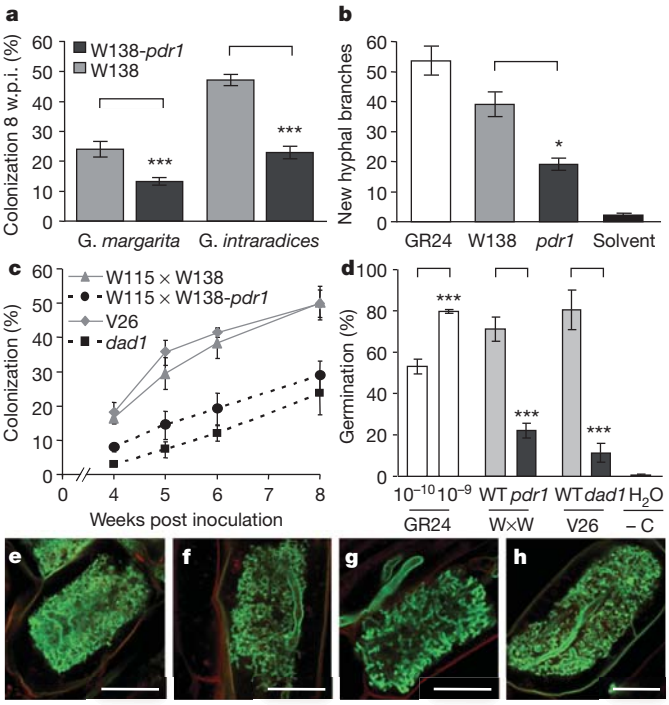

Figure 2 | Below-ground *pdr1* phenotypes. **a**, Arbuscular mycorrhizal colonization of W138 and W138-*pdr1* roots 8 w.p.i. with two arbuscular mycorrhizal fungi. Data are presented as mean ± s.e.m. ($n > 20$). **b**, *In vitro* branching response of *G. margarita* 24 h after application of GR24 ($n = 5$), root exudates from W138 ($n = 17$), root exudates from W138-*pdr1* ($n = 36$) or 10% acetone (solvent, $n = 5$). Data are presented as mean ± s.e.m. **c**, Kinetics of *G. intraradices* colonization of W115 × W138 ($n = 25$), W115 × W138-*pdr1* ($n = 25$), V26 ($n = 5$) and *dad1* mutants ($n = 5$). Data are presented as mean ± s.e.m. ($P < 0.001$ for all time points between mutants and wild types). **d**, *P. ramosa* germination induced by GR24 ($n = 3$), root exudates from W115 × W138 (W×W WT, $n = 10$), W115 × W138-*pdr1* (W×W *pdr1*, $n = 10$), V26 ($n = 4$), *dad1* mutants ($n = 4$) or water (H_2O, $n = 4$). Data are presented as mean ± s.e.m. – C, negative control. **e**–**h**, *G. intraradices* intracellular arbuscular mycorrhizal morphology 4 w.p.i. in W115 × W138 (**e**), W115 × W138-*pdr1* (**f**), V26 (**g**) and *dad1* mutants (**h**). Scale bars, 20 μm. **a**–**d**, *, $P < 0.05$; ***, $P < 0.001$.

differences in colonization were due to a decreased number of hyphal penetrations and retarded intraradical expansion of arbuscular mycorrhizal fungal colonies, rather than to defects in intracellular fungal development. Thus, the phenotype of *dad1* and *pdr1* mutants was distinct from that of arbuscular mycorrhizal mutants such as *pam1* (ref. 21), *str1* (ref. 22) or SYM-pathway[4] mutants, which commonly have aberrant arbuscular mycorrhizal fungal structures.

A detailed analysis of W138 root exudates resulted in the identification of the strigolactone orobanchol (Supplementary Fig. 6). The orobanchol levels in *pdr1* plant root exudates were significantly lower than those in wild-type plant exudates (Fig. 3a), whereas the levels in root extracts were not affected (Fig. 3b), indicating that *pdr1* mutants are not defective in strigolactone biosynthesis. Orobanchol was not detectable in root exudates or in root extracts of *dad1* plants, confirming this mutant's purported defect in strigolactone biosynthesis (Fig. 3a, b). The finding that only extraradical orobanchol levels were affected in *pdr1* mutants indicated that PDR1 functions as a strigolactone export carrier.

PDR1-dependent strigolactone transport was further explored in a heterologous system by stable and constitutive overexpression of *GFP*::*gPaPDR1* in *Arabidopsis* Col-0, resulting in *PDR1*-OE lines (Supplementary Fig. 7a, b). *Arabidopsis* does not form arbuscular mycorrhizae and exudes only minuscule quantities of strigolactones[23]. When grown on GR24-containing medium, *PDR1*-OE lines proved

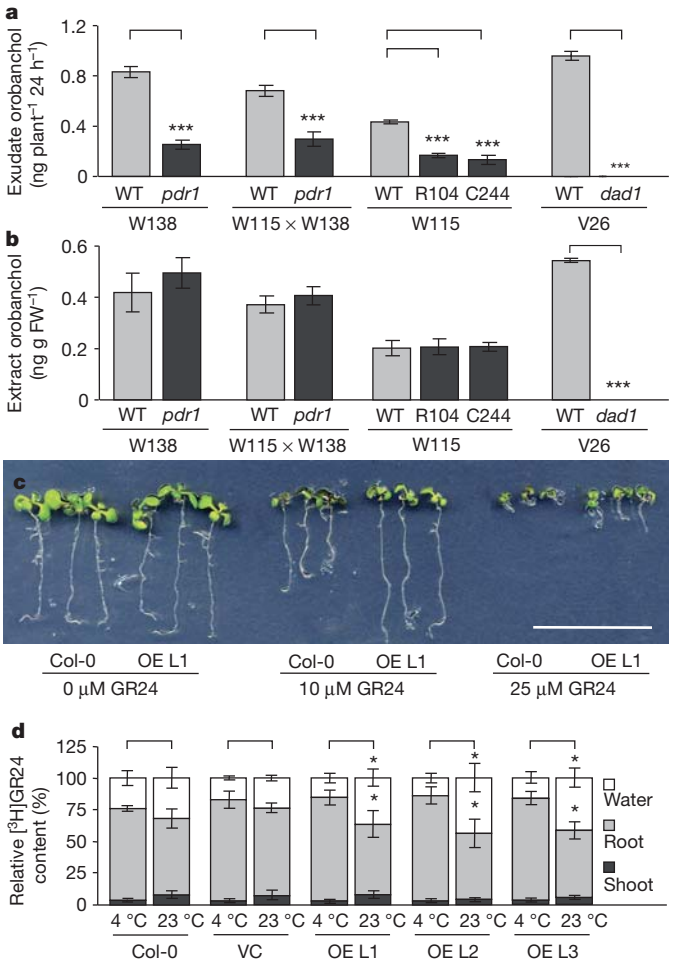

Figure 3 | Orobanchol content and PDR1-dependent GR24 tolerance and transport. **a**, **b**, Orobanchol in the root exudates (**a**) and extracts (**b**) of *pdr1* lines, *dad1* mutants and wild-type plants ($n = 9$). Data are presented as mean ± s.e.m. FW, fresh weight. **c**, Col-0 and *PDR1*-OE lines grown on 0, 10 and 25 µM GR24. Scale bar, 1 cm. **d**, GR24 export assay of [^{3}H]GR24-preloaded roots of Col-0, vector control (VC) and *PDR1*-OE lines (OE L1–3). Relative [^{3}H]GR24 in the medium (water), root and shoot after 1 h incubation at 4 °C and 23 °C. Data are presented as mean ± s.e.m. ($n = 8$). **a**, **b**, **d**, *, $P < 0.05$; ***, $P < 0.001$.

more tolerant to the deleterious effects of high strigolactone concentrations on root elongation[24] than did wild-type plants (Fig. 3c and Supplementary Fig. 7c). Direct strigolactone exudation was assessed by quantifying the efflux of preloaded [^{3}H]GR24 from roots either incubated at 4 °C, to monitor passive diffusion, or at 23 °C, allowing transporter-mediated efflux. After 1 h, *PDR1*-OE roots incubated at 23 °C retained significantly less GR24 than *PDR1*-OE roots incubated at 4 °C (Fig. 3d and Supplementary Fig. 7d). In agreement with this observation, more GR24 was found in the root exudates of *PDR1*-OE lines at 23 °C. No significant differences were found between the root extracts and root exudates of wild-type or vector control lines in either condition (Fig. 3d). These results, together with the observed GR24-resistance phenotype of *PDR1*-OE plants, are best explained by PDR1 acting as a strigolactone exporter.

Taken together, our data suggest a role for PDR1 in strigolactone secretion from HPCs. We propose that PDR1-mediated strigolactone exudation under low phosphate conditions creates local rhizosphere gradients that guide arbuscular mycorrhizal hyphae to HPCs, which are susceptible to hyphal penetration (Supplementary Fig. 1), thereby initiating arbuscular mycorrhizae. The symbiotic phenotype of *pdr1* and *dad1* mutants, and the induction of *PDR1* expression in colonized root segments, suggests that strigolactones play an additional role in promoting sustained intercellular root colonization, whereas intracellular stages (for example, arbuscules) develop independently of strigolactones (Fig. 2e–h).

Recently, it was demonstrated that strigolactones inhibit shoot branching[5,6]. Although certain aspects of strigolactone biosynthesis and signalling have been unravelled[25], information about the mode of strigolactone transport is scant. Strigolactones are mobile within the xylem sap[23], but it is not known how they are released from the producing cells and whether directed cell-to-cell transport occurs. Strigolactone biosynthesis is subject to direct negative feedback regulation[26]. Hence, strigolactone biosynthesis needs to be coordinated with export to prevent strigolactones from accumulating to levels that would restrict further production. Indeed, *PDR1* expression was found to be stimulated by exogenous application of GR24 (Figs 1c and 4a), suggesting that this gene is induced in a substrate-dependent manner, as previously observed for other PDR subfamily[9,15] members.

Above ground, *PDR1* expression was largely confined to stem tissues, particularly the vasculature and nodal tissues adjacent to leaf axils (Fig. 4b, c). However, *PDR1* expression was absent from dormant buds (Fig. 4d). This pattern is consistent with PDR1 functioning as

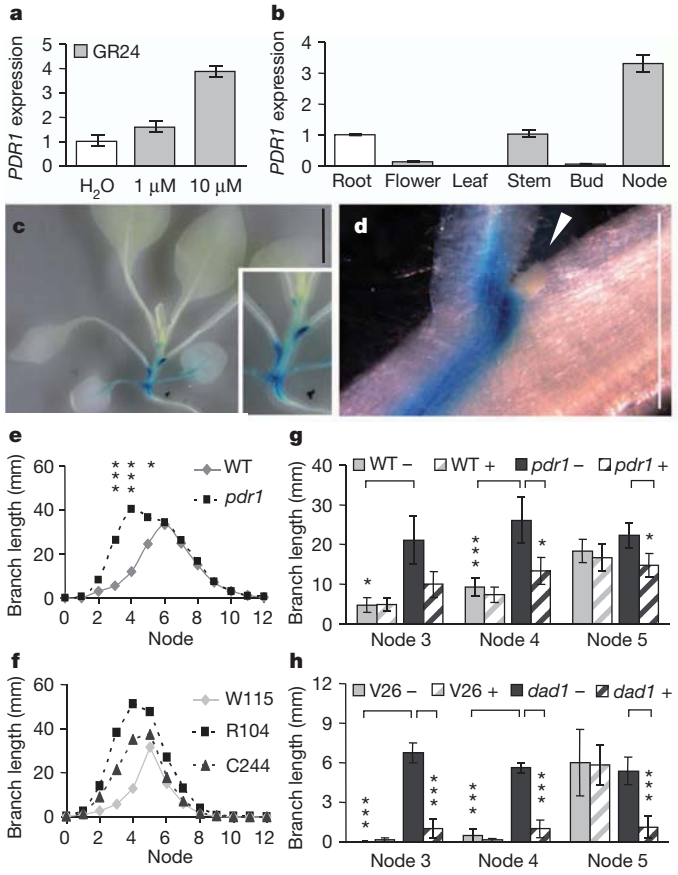

Figure 4 | Above-ground *PDR1* expression and *pdr1*-related branching phenotypes. **a**, **b**, Quantitative PCR for above-ground W115 GR24-treated tissue (**a**) and various organs (**b**). Data are presented as mean ± s.e.m. ($n = 3$). **c**, **d**, *pPhPDR1*::*GUS* in W115 at the four-leaf stage (**c**) and in the node (**d**) (white arrowhead, dormant axillary bud). The inset in **c** shows a magnification of the lower right corner of **c**. Scale bars, 10 mm (**c**) and 1 mm (**d**). **e**, **f**, Branch development 41 days post germination. Data are presented as mean ± s.e.m. Branch length is shown for W115 × W138 and W115 × W138-*pdr1* ($n = 110$) (**e**) and for W115 and two *pdr1*-RNAi lines, R104 ($P < 0.001$ for node 3–4) and C244 ($P < 0.05$ for node 3) ($n = 8$) (**f**). **g**, **h**, Effects of GR24 (+, striped bars) on branch development 34 days post germination at node 3–5 for W115 × W138 (WT) and W115 × W138-*pdr1* (*pdr1*) ($n = 24$) (**g**) and for V26 and *dad1* mutants ($n = 8$) (**h**). Data are presented as mean ± s.e.m. **a**, **b**, **e**, **h**, *, $P < 0.05$; ***, $P < 0.001$.

a strigolactone transporter. Although strigolactones are mobile in the xylem[23], a cellular transport system is required to deliver strigolactones to dormant buds that are not yet connected to the xylem. This idea is compatible with both current models of strigolactone-dependent branching control[27].

According to the 'second messenger model', strigolactones are transported to the bud as a second messenger of auxin[28], hence cellular transport of strigolactones in the axillary regions would be indispensable. In the 'auxin transport canalization-based model', strigolactones are thought to dampen polar auxin transport, resulting in the accumulation of auxin to levels that inhibit bud outgrowth[29]. Strigolactones could restrict auxin transport systemically and/or locally[27]. For both models, local strigolactone transport capacity near the axils would be in line with the inhibitory role of strigolactones on branching. In W115 × W138-*pdr1* plants, bud outgrowth was initiated sooner (Supplementary Fig. 8a) and more vigorously than in the wild-type plants, causing longer branches (Fig. 4e and Supplementary Fig. 8e–h) at node three to five. This early and vigorous bud outgrowth was also observed in *pdr1*-RNAi lines (Fig. 4f). *Dad1* mutants initiate branches from all nodes (Supplementary Fig. 8d), and although branch elongation is retarded compared with the wild type, these mutants eventually produce full branches from every node[20,30]. At flowering time, this results in a phenotype that is more pronounced than in any of the *pdr1* mutants, which have final branch patterns that differ only marginally from the respective wild-type plants (Supplementary Fig. 8b, c and Supplementary Table 1). Nevertheless, the *pdr1* mutant branching phenotype seems to be strigolactone-dependent and related to the *dad1* mutant branching phenotype, because branch elongation in both mutants could be suppressed to near wild-type conditions by exogenous application of GR24 to the leaf axils (Fig. 4g, h).

In conclusion, the identification of PDR1-mediated strigolactone transport contributes to a more comprehensive view of the modes of action of strigolactones. Understanding the underlying transport mechanisms is crucial for a holistic view of phytohormone function. Strigolactone transport has a direct effect on the phosphate-dependent control of arbuscular mycorrhizal levels and on the control of shoot branching, for which the integration of auxin and strigolactone signalling seems to be achieved partially through reciprocal transport modulation. The mild branching phenotype of *pdr1* mutants relative to the strigolactone-biosynthesis mutant *dad1* (ref. 30) suggests that residual transport and/or locally produced strigolactones may compensate for defective strigolactone transport in the shoot. However, arbuscular mycorrhizal development was affected to a similar degree in the *pdr1* and *dad1* mutants, revealing that below-ground strigolactone transport and secretion relies primarily on PDR1.

METHODS SUMMARY

All experiments, with the exception of the transport assays, were performed in accordance with established protocols. Detailed methods and associated references can be found in the Methods.

1. Cook, C. E., Whichard, L. P., Turner, B., Wall, M. E. & Egley, G. H. Germination of witchweed (*Striga lutea* Lour.): isolation and properties of a potent stimulant. *Science* **154,** 1189–1190 (1966).
2. Yoder, J. I. & Scholes, J. D. Host plant resistance to parasitic weeds; recent progress and bottlenecks. *Curr. Opin. Plant Biol.* **13,** 478–484 (2010).
3. Akiyama, K., Matsuzaki, K.-I. & Hayashi, H. Plant sesquiterpenes induce hyphal branching in arbuscular mycorrhizal fungi. *Nature* **435,** 824–827 (2005).
4. Parniske, M. Arbuscular mycorrhiza: the mother of plant root endosymbioses. *Nature Rev. Microbiol.* **6,** 763–775 (2008).
5. Umehara, M. *et al.* Inhibition of shoot branching by new terpenoid plant hormones. *Nature* **455,** 195–200 (2008).
6. Gomez-Roldan, V. *et al.* Strigolactone inhibition of shoot branching. *Nature* **455,** 189–194 (2008).
7. Petrasek, J. & Friml, J. Auxin transport routes in plant development. *Development* **136,** 2675–2688 (2009).
8. Kuromori, T. *et al.* ABC transporter AtABCG25 is involved in abscisic acid transport and responses. *Proc. Natl Acad. Sci. USA* **107,** 2361–2366 (2010).
9. Kang, J. *et al.* PDR-type ABC transporter mediates cellular uptake of the phytohormone abscisic acid. *Proc. Natl Acad. Sci. USA* **107,** 2355–2360 (2010).
10. Matusova, R. *et al.* The strigolactone germination stimulants of the plant-parasitic *Striga* and *Orobanche* spp. are derived from the carotenoid pathway. *Plant Physiol.* **139,** 920–934 (2005).
11. Verrier, P. J. *et al.* Plant ABC proteins — a unified nomenclature and updated inventory. *Trends Plant Sci.* **13,** 151–159 (2008).
12. Moons, A. Transcriptional profiling of the *PDR* gene family in rice roots in response to plant growth regulators, redox perturbations and weak organic acid stresses. *Planta* **229,** 53–71 (2008).
13. Badri, D. V. *et al.* An ABC transporter mutation alters root exudation of phytochemicals that provoke an overhaul of natural soil microbiota. *Plant Physiol.* **151,** 2006–2017 (2009).
14. Sugiyama, A., Shitan, N. & Yazaki, K. Signaling from soybean roots to rhizobium: an ATP-binding cassette-type transporter mediates genistein secretion. *Plant Signal. Behav.* **3,** 38–40 (2008).
15. Jasinski, M. *et al.* A plant plasma membrane ATP binding cassette-type transporter is involved in antifungal terpenoid secretion. *Plant Cell* **13,** 1095–1107 (2001).
16. Hayward, A., Stirnberg, P., Beveridge, C. & Leyser, O. Interactions between auxin and strigolactone in shoot branching control. *Plant Physiol.* **151,** 400–412 (2009).
17. Hanlon, M. T. & Coenen, C. Genetic evidence for auxin involvement in arbuscular mycorrhiza initiation. *New Phytol.* **189,** 701–709 (2011).
18. Sharda, J. N. & Koide, R. T. Can hypodermal passage cell distribution limit root penetration by mycorrhizal fungi? *New Phytol.* **180,** 696–701 (2008).
19. Koes, R. *et al.* Targeted gene inactivation in petunia by PCR-based selection of transposon insertion mutants. *Proc. Natl Acad. Sci. USA* **92,** 8149–8153 (1995).
20. Snowden, K. C. *et al.* The Decreased apical dominance1/*Petunia hybrida CAROTENOID CLEAVAGE DIOXYGENASE8* gene affects branch production and plays a role in leaf senescence, root growth, and flower development. *Plant Cell* **17,** 746–759 (2005).
21. Reddy, D. M. R. S., Schorderet, M., Feller, U. & Reinhardt, D. A petunia mutant affected in intracellular accommodation and morphogenesis of arbuscular mycorrhizal fungi. *Plant J.* **51,** 739–750 (2007).
22. Zhang, Q., Blaylock, L. A. & Harrison, M. J. Two *Medicago truncatula* half-ABC transporters are essential for arbuscule development in arbuscular mycorrhizal symbiosis. *Plant Cell* **22,** 1483–1497 (2010).
23. Kohlen, W. *et al.* Strigolactones are transported through the xylem and play a key role in shoot architectural response to phosphate deficiency in nonarbuscular mycorrhizal host *Arabidopsis*. *Plant Physiol.* **155,** 974–987 (2011).
24. Ruyter-Spira, C. *et al.* Physiological effects of the synthetic strigolactone analog GR24 on root system architecture in *Arabidopsis*: another belowground role for strigolactones? *Plant Physiol.* **155,** 721–734 (2011).
25. Beveridge, C. A. & Kyozuka, J. New genes in the strigolactone-related shoot branching pathway. *Curr. Opin. Plant Biol.* **13,** 34–39 (2010).
26. Mashiguchi, K. *et al.* Feedback-regulation of strigolactone biosynthetic genes and strigolactone-regulated genes in *Arabidopsis*. *Biosci. Biotechnol. Biochem.* **73,** 2460–2465 (2009).
27. Domagalska, M. A. & Leyser, O. Signal integration in the control of shoot branching. *Nature Rev. Mol. Cell Biol.* **12,** 211–221 (2011).
28. Brewer, P. B., Dun, E. A., Ferguson, B. J., Rameau, C. & Beveridge, C. A. Strigolactone acts downstream of auxin to regulate bud outgrowth in pea and *Arabidopsis*. *Plant Physiol.* **150,** 482–493 (2009).
29. Crawford, S. *et al.* Strigolactones enhance competition between shoot branches by dampening auxin transport. *Development* **137,** 2905–2913 (2010).
30. Napoli, C. highly branched phenotype of the petunia *dad1–1* mutant is reversed by grafting. *Plant Physiol.* **111,** 27–37 (1996).

Supplementary Information is linked to the online version of the paper

Acknowledgements We kindly thank the following: C. Gübeli for technical assistance; and T. Gerats, S. Hörtensteiner, A. Osbourne, P. Schläpfer and C. Beveridge for comments. This study was funded by the Swiss National Foundation within the NCCR-Plant Survival (project 'ABC transporters involved in signaling') and by The Netherlands Organization for Scientific Research (NWO; VICI grant 865.06.002 and Equipment grant 834.08.001to H.J.B.). H.J.B. was co-financed by the Centre for BioSystems Genomics (CBSG).

Author Contributions T.K. wrote the manuscript, designed the project and carried out most of the experiments. W.K. and R.B. carried out the *P. hybrida* strigolactone analysis and the *P. ramosa* biossays. J.S. performed the quantitative PCR with reverse transcription assays and the transport assays. J.S. and M.S. performed branching and GUS trials. L.B. analysed the *PDR1*-OE lines. J.B.B. sectioned material. D.R. investigated arbuscular mycorrhizal morphology. H.J.B. supervised the analytical part of the project. E.M. conceived and supervised the project. D.R., E.M., J.S., W.K. and H.J.B. assisted in editing the manuscript.

Author Information Sequences for *P. hybrida PDR1*, a 1.8-kb element upstream of *PDR1* and the *P. axillaris* orthologue of *PDR1* have been deposited in the GenBank database under accession numbers JQ292813, JQ292814 and JQ292812. Correspondence and requests for materials should be addressed to T.K.

METHODS

Plant growth conditions. Petunia lines were grown with a 16 h light cycle, at 60% relative humidity and 25 °C in soil (ED 73, Einheitserde) or in clay granules (Oil Dri US-Special, Damolin). Clay granules were supplemented once a week with half-strength Hoagland solution. For mycorrhization trials, a mix of 40% (v/v) soil, 40% (v/v) clay granules, 10% (v/v) sand and 10% (v/v) mycorrhizal inoculum (Agrauxine) was used. Seeds were plated on medium containing 2.2 g l^{-1} MS medium (Duchefa) and 15 g l^{-1} sucrose, supplemented with 9 g l^{-1} Phyto Agar (Duchefa), with a 16 h light cycle at 25 °C. *Arabidopsis* was grown in vertical plates on medium containing 2.2 g l^{-1} MS medium and 15 g l^{-1} sucrose, supplemented with 9 g l^{-1} Phyto Agar, with a 16 h light cycle and 60% relative humidity at 21 °C. For hormone treatment, 14-day-old W115 seedlings grown on plates were exposed for 24 h to final concentrations of 1 μM or 10 μM of the synthetic strigolactone analogue GR24 (Chiralix), 10 μM ABA or 25 μM NAA. For phosphate starvation, 14-day-old W115 seedlings were transferred to phosphate-free plates for 1 week.

***PDR1* cloning strategy.** *PDR*-specific 0.5-kb transcripts were amplified from W115 root cDNA 5 weeks post inoculation (w.p.i.) with *G. intraradices*, using the following primers: 5′-mgwatgactctdytkytkggacctcc-3′ and 5′-gyttcytytgncchc chgaaatwcc-3′ (5′ region), or 5′-gggwaaracggwgtyagtggwgcw-3′ and 5′-ctcatnaca atdgcwgcwgctctwgc-3′ (3′ region). Sequences follow the universal degenerate code. The resultant 5′ and 3′ fragments were aligned, and the deduced consensus primers 5′-TATTGGGACTTGAAATTTGTGCCGATAC-3′ and 5′-GCTCCACTAACAC CCATCAGAGCTGTC-3′ were used to amplify putative *PDR* fragments spanning 2.5 kb. The 5′ and 3′ ends of *P. hybrida PDR1* were amplified using a SMART RACE Amplification Kit (Clontech) with 5′ RACE (5′-CTCGAGTACATTTTCT CGGGGACCTTGG-3′), nested 5′ RACE (5′-CCATTTCGTCTCCAACAATG GTATCGG-3′), 3′ RACE (5′-GTCCTCAAGAGTAGGAAGCATCACTGCG-3′) and nested 3′ RACE (5′-ACCGAGGACCGGCTTGAACTCTTGAGAG-3′). The full-length *P. hybrida PDR1* cDNA GenBank accession number is JQ292813.

To obtain the full-length genomic sequence of *PDR1*, a *P. axillaris* BAC library (from C. Kuhlemeier) was screened with 5′-TGCCAATCCTTCATGATGTCA GTGG-3′ and 5′-CCTTCTCTCTCCTAGACAGCTCTGC-3′. *P. axillaris* is a progenitor of the hybrid species *P. hybrida*[31], and a genomic library for BAC-based cloning was available only for *P. axillaris*. BACs were extracted from candidate clones via the Large-Construct Kit (QIAGEN). Full-length genomic *P. axillaris PDR1* was amplified from a BAC with 5′-AATTACTAGTATGGAGGGTG GTGAAG-3′ and 5′-AATTGCATGCCTATCTTTTCTGGAAATTAAATG-3′, cut with SpeI and SphI, and cloned into the vector pUC18-GFP5Tsp through compatible NheI and SphI restriction sites, for use in GFP localization studies[32]. For stable transformation, the CaMV *35S::GFP::gPaPDR1*-terminator cassette was cloned from pUC18-GFP5Tsp into the pGreenII 0179 vector[33] by using the following strategy. First, the CaMV *35S* promoter from native pUC18-GFP5sp was cloned via XhoI and XmaI sites. Second, the terminator from the native pUC18-GFP5Tsp, including the upstream SphI site, was cleaved with NheI and SacI and inserted into CaMV *35S*-pGreenII 0179 via compatible XbaI and SacI sites. Third, *GFP::gPaPDR1* was cut and cloned via XmaI and SphI. Nine kilobases of the genomic *P. axillaris PDR1* locus, including upstream and downstream sequence, were submitted to GenBank under accession number JQ292812.

***PDR1* promoter GUS construct and GUS staining assay.** A 1.8-kb *P. hybrida PDR1* promoter fragment was amplified using a GenomeWalker Universal Kit (Clontech) with 5′-AGTTGGAAGTTTCTCAAGTGCAGCCCA-3′ and the nested 5′-CCCTAAAGAGTTCTTCACCACCCTCCAT-3′ (GenBank accession number JQ292814). The fragment was cloned into the pGEM-T-Easy Vector system (Promega), reamplified with 5′-CATGAAGCTTGCACCCAGAAGAAG ATTAGGC-3′ and 5′-TCGATCTAGACACATTAAGAGGAAAGTAGGTAC-3′ and cloned into the pGPTV-BAR[34] vector system via HindIII and XbaI. Of the original T0 transformants, eight lines were selected for further analysis. Segregating T1 individuals of all eight lines had comparable below-ground and above-ground expression patterns at different developmental stages. Two of these lines were chosen for the in-depth analysis presented in this work, and all data presented were confirmed in both lines.

GUS-staining trials were performed as described previously[35]. After staining, samples were cleared for 24 h in 10% (w/v) KOH and stored in 70% (v/v) ethanol. For the analysis of HPCs, 5-bromo-6-chloro-3-indolyl β-D-glucuronide cyclohexylammonium salt was used for GUS staining, and samples were cleared for 24 h in 10% (w/v) KOH before staining with trypan blue as described previously[18].

***PDR1* RNAi constructs.** Silencing of *P. hybrida PDR1*-specific transcripts was performed with the pKANNIBAL vector system[36]. Two constructs were designed: one targeting a highly variable region within nucleotide binding domain 2 (NBD2) of *PDR1* (the C construct), and the other targeting part of the 3′ end and the 3′ untranslated region of *PDR1* (the R construct). The 148-base-pair (bp) C fragment (5′-GGAACGCAAGCAAAAGGGGTGAGGTTATTGAACTATCTTCGCTTGG AAAGAGCTCTTCTGAAAAAGGAAATGATGTTCGGCGAAGTGCATCTTC CAGGTCAATGTCCTCAAGAGTAGGAAGCATCACTGCGGCTGATTTGAG CAAGAG-3′) was amplified from W115 cDNA with 5′-CGATGGATCCTCGA GGGAACGCAAGCAAAAGGG-3′, containing BamHI and XhoI restriction sites and with 5′-CGATATCGATGGTACCCTCTTGCTCAAATCAGCCGCAGTGA-3′ containing ClaI and KpnI sites. The 411-bp R fragment (5′-GACATTATATG GACTAATTGCCTCACAATTTGGAGACATACAAGACAGACTTGACACAA ATGAGACAGTGGAACAATTCATAGAGAATTTCTTTGATTTCAAACATG ATTTTGTGGGATATGTTGCTCTCATTCTTGTTGGGATTTCTGTTCTTTT TCTCTTCATTTTTGCATTTTCAATTAAAACATTTAATTTCCAGAAAAGA TAGGTTGGTCCAGGTATACACATGAAAAGAGCGTTTATCAAGATATGT GTATATTAGGATAATAATATAATCTTTCTTTTTCCTCTTTTTTACTTATT GTGGTTTTCTCAAGTTTGGAATAGATAGAACCAAAAGTCTGTACTCTG TATTTAAGAACAACTTTTGTACACATTGTTATGTATTGGAGAAGTTATG AGTATCTTTTG-3′) was amplified with 5′-CGATGGATCCTCGAGACATTA TATGGACTAATTGCC-3′ containing BamHI and XhoI restriction sites and with 5′-CGATATCGATGGTACCAAAAGATACTCATAACTTCTCC-3′ containing ClaI and KpnI sites. The resultant amplicons were cloned in the sense and antisense direction in the two multiple cloning sites of pKANNIBAL. The pKANNIBAL RNAi cassette was excised from the vector backbone via NotI and transferred into the binary pGreenII 0229 vector[33]. After stable transformation of W115, the extent of downregulation was estimated by semiquantitative PCR or PCR with reverse transcription.

Plant transformation. W115 was transformed as described previously[37]. Construct insertion was confirmed by PCR on genomic DNA with the primers 5′-ACGGTCCACATGCCGGTATATACGATG-3′ and 5′-GATGGCATTTGTA GGAGCCACCTTCC-3′, which target the CaMV *35S* promoter, or with 5′-GAA TTGATCAGCGTTGGTGGGAAAGC-3′ and 5′-GGTAATGCGAGGTACGGT AGGAGTTG-3′, which target the *GUS* gene.

Transient transformation of *Arabidopsis* Col-0 protoplasts was performed as described previously[32]. *Arabidopsis* plants were stably transformed as described previously [38]. The T0 generation was selected for hygromycin resistance. Plants of the T1 generation were tested for hygromycin resistance and GFP expression.

Screening approach to identify transposon insertions in *PDR1*. A 3D-gDNA library (from T. Gerats) representing 10 × 10 × 10 (1,000) W138 individuals was screened for dTph*1* insertions in *P. hybrida PDR1* using a PCR-based method[39]. The entire genomic region of *PDR1* was scanned in contiguous steps covering less than 1 kb, using the dTph*1*-specific primer 5′-GAATTCGCTCCGCCCCTG-3′ and a variety of ^{33}P-labelled gene-specific primers. The primer 5′-CCATTTCGTC TCCAACAATGGTATCGG-3′ yielded a positive result. Homozygosity PCRs were performed with transposon-flanking primers: 5′-tgccaatccttcatgatgtcagtgg-3′ and 5′-ccttctctctcctagacagctctgc-3′. Homozygous dTph*1* insertion alleles were crossed into W115, the progeny were selfed, and the resultant offspring were tested for homozygosity with the abovementioned primers. Transposon display analysis using six W115 × W138 and five W115 × W138-*pdr1* lines was performed as described previously[40].

Mycorrhization trials. Subsets of mycorrhized roots were stained[41] and quantified for their level of colonization using the gridline intersect method[42]. Only roots with clear intraradical structures such as coiled cortical hyphae, arbuscules and vesicles were scored as positively mycorrhized. A minimum of 200 intersecting root fragments per sample were investigated microscopically for intraradical arbuscular mycorrhizal structures. For trials involving W115 × W138 lines, five individuals from five lines were analysed, and the data were presented as a pool of $n = 25$ (5 × 5). Double staining of the colonized roots with propidium iodide and wheat germ agglutinin coupled to fluorescein isothiocyanate (WGA-FITC, Sigma-Aldrich) was performed as described previously[43].

Hyphal branching bioassays. Branching assays were performed as described previously[44] with preselected spores of *G. margarita* (Agrauxine). For the production of the root exudate concentrate, petunia lines were grown in clay granules and then transferred for 24 h to 0.1 l of a hydroponic solution containing 2 mM $CaCl_2$ and 2 mM KSO_4 and kept under constant aeration. The hydroponic solution was then passed through a Sep-Pak Classic C18 Cartridge (Waters) to adsorb hydrophobic root exudates. Exudates were eluted from the column using 2 ml of acetone, and the eluent was dried over nitrogen. Dried exudates were redissolved in acetone and normalized according to root fresh weight. Exudate equivalents of 10 mg root fresh weight were used in each branching assay.

Transport assays and GR24 tolerance assays. *Arabidopsis* seeds from three independent *PDR1*-OE lines were surface-sterilized with 1% (v/v) bleach and 50% (v/v) ethanol and plated on media supplemented with 2.2 g l^{-1} MS medium, 1% (w/v) sucrose and 0, 10 or 25 μM GR24. After three days of stratification, plants were moved to a 16 h light cycle and selected for GFP fluorescence after 3 days of growth. Root length was determined with ImageJ 1.44 software (http://rsbweb.nih.gov/ij) after 7 days, and seedlings were moved to hygromycin-containing plates without sucrose to confirm the selection by GFP fluorescence.

For transport experiments, seeds were sterilized in the same way and plated on hygromycin-containing medium. After 3 days of stratification and 3 days of growth, seedlings were checked for GFP fluorescence. After 7 days, GFP- and hygromycin-positive plants were transferred to medium supplemented with 2.2 g l^{-1} MS medium and 1% (w/v) sucrose and grown for another 7 days. Three *PDR1*-OE lines, Col-0 and a vector control line were incubated for 2 h in the dark at 4 °C with root tips submerged in 0.1% (w/v) Phyto Agar supplemented with 25 nM [^{3}H]GR24 (specific activity 40 Ci $mmol^{-1}$; American Radiolabeled Chemicals). Subsequently, the plant roots were washed in ice-cold 1 mM $CaCl_2$ and incubated in 200 µl 0.1% Phyto Agar. For each line, 50% of the plants were kept for a further 1 h at 4 °C in the dark as a diffusion control, and the other 50% were shifted to 23 °C for 1 h to monitor transport. Subsequently, the shoot, root and Phyto Agar fractions were incubated for 30 min in 50 µl 24% (w/v) trichloroacetic acid at 23 °C. ^{3}H counts were determined in 3 ml ULTIMA Gold LSC cocktail (Perkin Elmer) with a Liquid Scintillation Analyser Tri-Carb 2900TR (Packard BioScience). The number of disintegrations per minute was computed into a percentage for each fraction and normalized to tissue fresh weight.

RNA isolation, cDNA synthesis, semiquantitative PCR and quantitative RT–PCR. RNA was isolated with an RNeasy Plant Mini Kit (QIAGEN). Reverse transcription of RNA to cDNA was performed with M-MLV Reverse Transcriptase (Promega) and a poly(T) primer (Promega).

P. hybrida PDR1 expression was quantified semiquantitatively with the primers 5′-GAAACTGTGGCCGAAAGG-3′ and 5′-GAGTTCAAGCCGGTCCT-3′ or 5′-AAATGCTACTACAGTGCAG-3′ and 5′-CATATAATGTCCAGGAAATG GG-3′. Tubulin 1 (*TUB*) transcripts, partially amplified with 5′-CATTG GTCAAGCCGGTTATTC-3′ and 5′-ACCCTTGAAGACCAGTACAGT-3′, served as a housekeeping and loading control.

Samples were diluted 1:30, and the diluted samples (4 µl) were added to each reaction well, serving as template for the reaction. Deionized water served as a negative control for amplification. *PDR1* expression was quantified with the primers 5′-CCTGAGGTTTACCAAATGGG-3′ and 5′-GATGGTATTGGATTGGAGCA-3′. Glyceraldehyde 3-phosphate dehydrogenase (*GAPDH*) expression was quantified with the primers 5′-GACTGGAGAGGTGGAAGAGC-3′ and 5′-CCGTTAAG AGCTGGGAGAAC-3′. *GAPDH* served as a housekeeping gene for normalization because it has been shown not to be regulated by hormonal treatments or mycorrhization (D. Reinhardt, personal communication). Final primer concentrations of 50, 100, 200 and 300 nM were tested for cDNA amplification and melting behaviour in the range of 60 °C to 95 °C. Because no differences were recorded, the average concentration of 100 nM was chosen for further experiments. Primer efficiency was recorded with W115 root cDNA as a template in a dilution range of 1:1 to 1:512, resulting in 94.42% for *P. hybrida PDR1* and 98.561% for *GAPDH*. These values were taken into account in the calculations. SYBR Green PCR Master Mix (Applied Biosystems) was added to the samples to a 20 µl final volume. For each sample, three technical replicates were pipetted. RT–PCR was performed on a 7500 Fast Real-Time PCR System (Applied Biosystems) with 7500 Software version 2.0.4. For quantification, comparative C_T ($\Delta\Delta C_T$) was chosen as the method[45]; the PCR run was divided into three parts: first, the hold stage (50 °C for 2 min and 95 °C for 10 min); second, the cycling stage (95 °C for 15 s and 60 °C for 1 min for 40 cycles); and third, the melt curve stage (95 °C for 15 s, 60 °C to 95 °C over 1 min, 95 °C for 30 s, and 60 °C for 15 s). Relative differences were calculated as described previously[45,46]. Each experiment was performed for three biological replicates.

Isolation, identification and quantification of petunia strigolactones. Plants were grown in an X-Stream 20 aeroponic system (Nutriculture) as previously described for *Medicago truncatula*[47]. From day 8 until day 12, exudates were collected and pooled, and root material was sampled. Samples were stored at −80 °C until analysis. *P. hybrida* root exudates and extracts were prepared and analysed by ultra performance liquid chromatography coupled to tandem mass spectrometry (UPLC-MS/MS) as previously described for *Arabidopsis*[22]. Orobanchol was provided by K. Yoneyama. For trials involving W115 × W138 lines, three individuals from three lines were analysed, and the data are presented as a pool of $n = 9$ (3 × 3).

***P. ramosa* germination bioassay.** Germination assays with *P. ramosa* seeds were conducted as reported previously[10]. Exudates were prepared as described above (in the subsection 'Hyphal branching bioassays'). GR24 (0.1 or 1.0 nM) and demineralised water were included as positive and negative controls, respectively. *P. ramosa* seeds were provided by M. Vurro. For trials involving W115 × W138 lines, two individuals from five lines were analysed, and the data are presented as a pool of $n = 10$ (5 × 2).

Trypan blue staining of HPCs. Trypan blue staining of HPCs in roots was performed as described previously[18].

Axillary branching trials. For a comparative analysis of lateral branch production in wild-type and *pdr1* backgrounds, plants were grown for 65 days in 0.55 l pots in soil as described above (in the subsection 'Plant growth conditions') and were watered daily. Branch development was monitored at different time points in a binominal fashion (yes/no) with respect to the following parameters: bud length >7 mm and full branch. Full branches were scored in accordance to a petunia branch definition[48]. Furthermore, branch length was scored as a continuous parameter. For trials involving W115 × W138, 22 individuals from 5 lines were analysed, and the data are presented as a pool of $n = 110$ (5 × 22). For branch length trials in response to GR24 treatments, three lines each of W115 × W138, W115 × W138-*pdr1*, V26 and the *dad1* mutant (from K. Snowden) were grown in soil as described above (in the subsection 'Plant growth conditions'). From 25 to 40 days post germination, plants were treated three times each week with 0 µM or 10 µM GR24 as described previously[6]. For trials involving W115 × W138 lines, eight individuals from three lines were analysed, and the data are presented as a pool of $n = 24$ (3 × 8).

Statistical analyses. Depending on the experimental set-ups and prerequisites, Students *t*-tests, Fisher's Exact tests or generalized linear models (GLMs) with quasi-binominal error structures were applied using R software.

Bioinformatics. Analysis of DNA fragments and vector constructs was performed using Vector NTI software (Invitrogen). The membrane topology of PDR1 was predicted using ConPredII[49]. Phylogenetic analysis of PDR1 was performed using tools available at Phylogeny.fr (http://www.phylogeny.fr). Alignments were performed with MultAlin software (http://multalin.toulouse.inra.fr/multalin/).

Robustness of data sets. All data sets presented were confirmed in at least two independent trials with similar set-ups and outcomes. For mycorrhization and branching trials, individual pots were randomized to reduce positional effects, and sample size was kept high to reduce background effects.

31. Zhang, X., Nakamura, I. & Mii, M. Molecular evidence for progenitorial species of garden petunias using polymerase chain reaction–restriction fragment length polymorphism analysis of the *Chs-j* gene. *HortScience* **43,** 300–303 (2008).
32. Meyer, A., Eskandari, S., Grallath, S. & Rentsch, D. AtGAT1, a high affinity transporter for γ-aminobutyric acid in *Arabidopsis thaliana*. *J. Biol. Chem.* **281,** 7197–7204 (2006).
33. Hellens, R. P., Edwards, E. A., Leyland, N. R., Bean, S. & Mullineaux, P. M. pGreen: a versatile and flexible binary Ti vector for *Agrobacterium*-mediated plant transformation. *Plant Mol. Biol.* **42,** 819–832 (2000).
34. Becker, D., Kemper, E., Schell, J. & Masterson, R. New plant binary vectors with selectable markers located proximal to the left T-DNA border. *Plant Mol. Biol.* **20,** 1195–1197 (1992).
35. Cervera, M. Histochemical and fluorometric assays for *uidA* (GUS) gene detection. *Methods Mol. Biol.* **286,** 203–213 (2004).
36. Wesley, S. V. *et al.* Construct design for efficient, effective and high-throughput gene silencing in plants. *Plant J.* **27,** 581–590 (2001).
37. Lutke, W. K. Petunia (*Petunia hybrida*). *Methods Mol. Biol.* **344,** 339–349 (2006).
38. Harrison, S. *et al.* A rapid and robust method of identifying transformed *Arabidopsis thaliana* seedlings following floral dip transformation. *Plant Methods* **2,** 19 (2006).
39. Vandenbussche, M. & Gerats, T. TE-based mutagenesis systems in plants: a gene family approach. *Methods Mol. Biol.* **260,** 115–127 (2004).
40. Van den Broeck, D. *et al.* Transposon display identifies individual transposable elements in high copy number lines. *Plant J.* **13,** 121–129 (1998).
41. Vierheilig, H., Coughlan, A., Wyss, U. & Piche, Y. Ink and vinegar, a simple staining technique for arbuscular-mycorrhizal fungi. *Appl. Environ. Microbiol.* **64,** 5004–5007 (1998).
42. Giovannetti, M. & Mosse, B. An evaluation of techniques for measuring vesicular arbuscular mycorrhizal infection in roots. *New Phytol.* **84,** 489–500 (1980).
43. Feddermann, N. *et al.* The *PAM1* gene of petunia, required for intracellular accommodation and morphogenesis of arbuscular mycorrhizal fungi, encodes a homologue of VAPYRIN. *Plant J.* **64,** 470–481 (2010).
44. Nagahashi, G. & Douds, D. D. Rapid and sensitive bioassay to study signals between root exudates and arbuscular mycorrhizal fungi. *Biotechnol. Techniques* **13,** 893–897 (1999).
45. Livak, K. J. & Schmittgen, T. D. Analysis of relative gene expression data using real-time quantitative PCR and the $2^{-\Delta\Delta CT}$ method. *Methods* **25,** 402–408 (2001).
46. Yuan, J. S., Reed, A., Chen, F. & Stewart, C. N. Statistical analysis of real-time PCR data. *BMC Bioinformatics* **7,** 85 (2006).
47. Liu, W. *et al.* Strigolactone biosynthesis in *Medicago trunculata* requires the symbiotic GRAS-TYPE transcription factors NSP1 and NSP2. *Plant Cell* **23,** 3853–3865 (2011).
48. Snowden, K. C. & Napoli, C. A. A quantitative study of lateral branching in petunia. *Funct. Plant Biol.* **30,** 987–994 (2003).
49. Arai, M. *et al.* ConPred II: a consensus prediction method for obtaining transmembrane topology models with high reliability. *Nucleic Acids Res.* **32,** 390–393 (2004).